International Journal of Greenhouse Gas Control 108 (2021) 103327

Contents lists available at ScienceDirect

International Journal of Greenhouse Gas Control

journal homepage: www.elsevier.com/locate/ijggc

# Modeling $CO_2$ separation on amine-containing facilitated transport membranes (AFTMs) by linking effects of relative humidity, temperature, and pressure

Qiang Yang [a], Qianguo Lin [b,c,*], Xi Liang [c,**]

[a] China-UK Low Carbon College, Shanghai Jiao Tong University, 201306, Shanghai, China
[b] International Energy Research Center, Shanghai Jiao Tong University, Shanghai, 200240, China
[c] Business School, The University of Edinburgh, Edinburgh, United Kingdom

ARTICLE INFO

*Keywords:*
Membrane gas separation
Amine-containing facilitated transport membranes
Variable gas permeance
Relative humidity
Modeling

ABSTRACT

Amine-containing facilitated transport membranes (AFTMs) hold great potential in $CO_2$ separation and show remarkable separation performance under the existence of water. Conventional membrane gas separation models that mainly consider the effect of temperature and pressure are less effective for modeling AFTMs. In this study, we present a model that involves variable $CO_2$ permeance in AFTMs concerning relative humidity (RH), temperature, and $CO_2$ partial pressure. Sensitivity analysis and comparison of the proposed model and simplistic model highlight the significance of considering the effect of RH and $CO_2$ partial pressure on gas permeance of AFTMs. Case study results of post-combustion carbon capture indicate that variations in $CO_2$ concentration and feed pressure bring more pronounced changes on the separation performance of AFTMs than in temperature. Besides, the results of RH along the membrane module provide evidence of membrane area for module design with required RH, and the results can also be used to guide the humidification of multistage separation processes using AFTMs. Overall, the proposed model can be integrated into commercial process simulators to study the separation process with consideration of variations in operating conditions within the membrane module, overcoming the lack of rigorous models for supporting the design of membrane systems for carbon capture.

## 1. Introduction

$CO_2$ separation is receiving increasing research attention over the past years as it is an important means for industrial gas treatment processes as well as mitigating global climate change (N.Borhani and Wang, 2019; Guandalini et al., 2019; Siagian et al., 2019). Current $CO_2$ separation technologies in many industrial gas treatment processes are absorption, adsorption, and cryogenic distillation (Song et al., 2018). These technologies have been developed for decades and are applied successfully in industrial applications. However, more efforts are required to be made as those technologies are energy-intensive and cost-ineffective (Rodrigues et al., 2018; Ohs et al., 2019; Song et al., 2019). As a potential alternative, membrane gas separation technology received considerable attention within the past few years due to its advantages such as low cost, easy to scale-up, operation simplicity, and environmental friendliness (Tomé et al., 2015). Among different kinds of membrane that have been developed for $CO_2$ separation, amine-containing facilitated transport membranes (AFTMs) are promising as the transport of $CO_2$ can be enhanced by the amine carriers via facilitated transport mechanism (Han and Ho, 2018), allows to overcome the trade-off between permeability and selectivity, known as Robeson upper bound (Robeson, 2008). Besides, AFTMs favor the wet flue gases as they experience higher reaction kinetic of facilitated transport with the formation of hydrogen carbonate ion by the presence of $H_2O$ (Wang et al., 2017), which is suitable for many industrial gas treatment applications as the exhausted gases contain saturated water (Brunetti et al., 2010).

Mathematical modeling is an essential tool for engineering design and process optimization of membrane gas separation. Accurate estimation of gas permeance is of great importance for the advancement of modeling membrane gas separation. Over the years, mathematical modeling efforts have been focused on describing the AFTMs. Paul and Koros (Paul and Koros, 1976) derived a permeance equation by the

* Corresponding author at: International Energy Research Center, Shanghai Jiao Tong University, Shanghai, 200240, China.
** Corresponding author.
*E-mail addresses:* qianguo.lin@gmail.com (Q. Lin), xi.liang@ed.ac.uk (X. Liang).

https://doi.org/10.1016/j.ijggc.2021.103327
Received 6 December 2020; Received in revised form 2 March 2021; Accepted 29 March 2021
Available online 7 April 2021
1750-5836/

**Nomenclature**

*Symbols*

| | |
|---|---|
| $A$ | Membrane segment area ($m^2$) |
| $A_m$ | Total membrane area ($m^2$) |
| $C_p$ | Molar heat capacity ($kJ/kmol^{-1}\cdot℃^{-1}$) |
| $C_X$ | Carrier concentration($mol\ cm^{-3}$) |
| $D_{CO_2}$ | $CO_2$ diffusion coefficient ($cm^2\cdot s^{-1}$) |
| $D_{CO_2-X}$ | $CO_2$−carrier complex diffusion coefficient ($cm^2\cdot s^{-1}$) |
| $E_p$ | Gas permeation activation energy (kJ/mol) |
| $F$ | Molar flow rate (mol/h) |
| $H$ | Enthalpy (J) |
| $H_{co_2}$ | Henry's law constant of $CO_2$ ($MPa\ cm^3\ mol^{-1}$) |
| $J$ | Permeation flux ($m^3$/h) |
| $JT$ | Joule-Thompson |
| $K$ | Reaction equilibrium constant |
| $l$ | Membrane selective layer thickness (cm) |
| $L$ | Volume flow rate on the retentate ($m^3$/h) |
| $p_{CO_2}$ | $CO_2$ partial pressure |
| $P_h$ | Pressures on the feed side (bar) |
| $P_l$ | Pressures on the permeate side (bar) |
| $P_{sat}$ | Water saturated pressure (kPa) |
| $Q$ | Gas permeance ($m^3$ (STP) $m^{-2}\ h^{-1}\ bar^{-1}$) |
| $Q_c$ | Conductive heat transfer (J) |
| $r$ | Pressure ratio |
| $R$ | Molar gas constant ($8.314\ J\ mol^{-1}\ K^{-1}$) |
| $Re$ | Overall recovery (%) |
| $RH$ | Relative humidity (%) |
| $T$ | Temperature (K or ℃) |
| $V$ | Volume flow rate on the permeate ($m^3$/h) |
| $W$ | Gas work during separation (J) |
| $x$ | Gas mole fractions on the feed side |
| $y$ | Gas mole fractions on the permeate side |
| $y_{purity}$ | Product $CO_2$ purity (%) |

*Greek symbols*

| | |
|---|---|
| $\alpha$ | Separation selectivity |
| $\theta$ | Stage cut |
| $\mu$ | Joule-Thompson coefficient (℃/bar) |

*Subscripts*

| | |
|---|---|
| $i$ | $i$-th component |
| $in$ | Feed side |
| $j$ | $j$-th component |
| $mix$ | Gas mixtures |
| $k$ | $k$-th membrane segment |
| $N$ | Number of membrane segments |
| $p$ | Permeate side |
| $R$ | Retentate side |

*Acronyms*

| | |
|---|---|
| AFTMs | Amine-containing facilitated transport membranes |
| $CH_4$ | Methane |
| $CO_2$ | Carbon Dioxide |
| $H_2O$ | Water |
| $N_2$ | Nitrogen |
| PVA | Polyvinyl alcohol |
| PVAm | Polyvinylamine |
| STP | Standard temperature and pressure |

partial immobilization model, the model can reflect the permeability decrease with partial pressure decrease. Ebadi Amooghin et al. (Ebadi Amooghin et al., 2018) modeled the $CO_2$ facilitated transport in AFTMs by the finite element method, the effect of partial pressure on gas permeation was considered, modeling results were in good agreement with experimental data. Scholz et al. (Scholz et al., 2013) developed a model to study the effect of temperature and pressure on membrane gas separation performance. Hosseini et al. (Hosseini et al., 2016) also presented a comprehensive model for membrane gas separation in which temperature and pressure effects can be taken into account. However, these models do not include the effect of water vapor in the flue gas on separation performance. Recently, Li et al. (Li et al., 2014) developed a facilitated transport model for AFTMs through reaction kinetics based on the reaction of $CO_2$ with amine carriers under the existence of $H_2O$. However, they did not include the effect of water vapor in the gas permeance. Pfister et al. (Pfister et al., 2017) conducted a comparative analysis of dry versus humid flue gas on polymeric glassy membrane and AFTMs to study the water vapor effect on $CO_2$ separation. Gas permeance under high relative humidity (RH) was used in the simulation for AFTMs. However, the model did not present the gas permeance equation as a function of RH, instead, the model used constant gas permeance. For AFTMs, gas separation performance is strongly dependent on RH apart from the temperature and pressure (Tong et al., 2015). Thus, it is necessary to include the effect of RH into the gas permeance estimation.

Moreover, high separation performance requires not only advanced membrane materials but also modularized membrane systems. In terms of membrane modules applied in large-scale membrane gas separation applications, temperature and pressure drop within the membrane module normally occur. Pressure drop occurs between the feed side and the retentate side of a membrane module (Hosseini et al., 2016). The $CO_2$ partial pressure decreases along the membrane due to the permeation of $CO_2$. The temperature of the permeate side would decrease as a result of the Joule-Thompson (JT) effect (Ahmad et al., 2013), while the temperature decrease occurs from the feed side to the retentate side is a direct consequence of heat transfer along with the gas permeation across the membrane (Rautenbach and Dahm, 1987). Ahmad et al.(Ahmad et al., 2013) proposed a cross-flow model for the hollow fiber membrane to describe the effect of temperature and pressure on membrane gas permeance, the variable gas permeance dependent on temperature and pressure is included in the model. However, their model did not consider the effect of water vapor content and its variation effect on gas permeance. In our recent work (Yang et al., 2020), we developed a model that considered the effect of water vapor content on gas permeance, the gas permeance is described as a function of gas RH. Whereas isothermal condition was assumed and pressure drop along the membrane was taken to be negligible, the model considered exclusively the effect of RH variation on gas permeance.

Therefore, the existing models may not give an effective estimation of a separation process using AFTMs. This study aims to address the lack of a suitable model for AFTMs by developing a model considering the simultaneous effect of RH, temperature, and $CO_2$ partial pressure for AFTMs. The effect of these parameters on gas permeance as well as separation performance was studied through sensitivity analysis and comparison of the proposed model and simplistic model. Moreover, variations of operating parameters along the membrane and its effect on separation performance were also taken into consideration through a case study of post-combustion carbon capture.

## 2. Model development

In this study, the calculation of multicomponent gas separation is done by applying the mathematical model derived by Shindo and coworkers (Shindo et al., 1985). The model has been validated with experimental data in previous studies (Pan, 1983; Xu et al., 2019a). Unlike their model, this study considers variable gas permeance.

Tanks-in-series approach (Coker et al., 1998; Bouton and Luyben, 2008; Katoh et al., 2011; Lee et al., 2017) is adopted to reflect the variable gas permeance as well as the variation of gas compositions along the membrane module. The cross-flow pattern is chosen for simulation as Yang et al. (Yang et al., 2017) compared the membrane gas separation results of three flow patterns (cross-flow, co-current flow, and counter-current flow), the difference between these three flow patterns is quite limited, and cross-flow is widely used for many applications. Fig. 1 schematically demonstrates a cross-flow model using the tanks-in-series approach for the spiral-wound membrane module.

Since the main objective of this study is to model the impacts of RH, temperature, and pressure on variable $CO_2$ permeance and separation performance, modeling governing equations are derived based on several assumptions to avoid an excessively complex modeling stage. The assumptions for the proposed model are as follows (Shao et al., 2012; Soroodan Miandoab et al., 2020):

1 The membrane operates at steady-state;
2 The thickness of the membrane dense layer remains constant along the membrane during the separation process.
3 Concentration polarization is negligible.

Modeling governing equations are based on our previous study (Yang et al., 2020). The difference from the previous study is that the effects of RH, temperature, and partial pressure are simultaneously included here. Appendix in this article provides detailed information for model development. The model equations can be implemented in MATLAB and solved by Newton iterative method with an initial guess of permeate gas composition. Determination of gas permeance equation that enables to reflect the effects of RH, temperature, and $CO_2$ partial pressure together can be seen in the following sections.

### 2.1. RH, temperature, and partial pressure-dependent gas permeance

In AFTMs, the transport of $CO_2$ follows facilitated transport mechanisms, while other non-reactive gas components (such as $N_2$, $H_2$, $CH_4$) follow the solution-diffusion mechanism. In the absence of $H_2O$, reactions between $CO_2$ and sterically unhindered amines follow a zwitterion mechanism (Caplow, 1968; Danckwerts, 1979). As described by Eqs. (1) and (2), one amine reacts with $CO_2$ to form a zwitterion intermediate, the zwitterion intermediate reacts with another amine subsequently to generate a carbamate (Ansaloni et al., 2015). In total, one $CO_2$ requires two amines to transport from the feed side to the permeate side of the membrane.

$$RR'NH + CO_2 \leftrightarrow RR'NH^+COO^- \tag{1}$$

$$RR'NH^+COO^- + RR'NH \leftrightarrow RR'NCOO^- + RR'NH_2^+ \tag{2}$$

Combining Eq. (1) and (2), yields Eq. (3):

$$2RR'NH + CO_2 \leftrightarrow^{K_1} RR'NCOO^- + RR'NH_2^+ \tag{3}$$

The $CO_2$ permeance equation based on the above reversible chemical reactions can be demonstrated as follows (Friedlander and Keller, 1965):

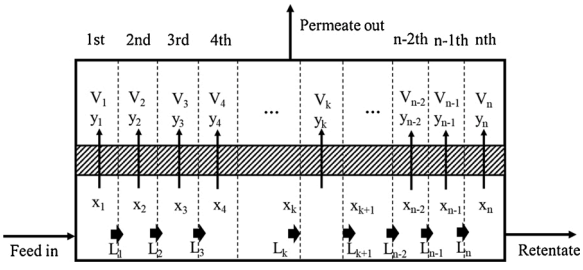


**Fig. 1.** Cross-flow model using tanks-in-series approach.

$$Q_1(p_{CO_2,0}) = \frac{D_{CO_2}}{lH_{co_2}} + \frac{D_{CO_2-X}C_XK_1}{l\left(2K_1p_{CO_2,0} + \sqrt{K_1H_{co_2}p_{CO_2,0}}\right)} \tag{4}$$

while in the presence of $H_2O$, $H_2O$ makes the carbamate unstable to form bicarbonate, as described in Eq. (5).

$$RR'NCOO^- + H_2O \leftrightarrow HCO_3^- + RR'NH \tag{5}$$

Combining Eq. (1), (2), and (5), yield Eq. (6). As a result, one $CO_2$ requires one amine to transport to the permeate side of the membrane.

$$RR'NH + CO_2 + H_2O \leftrightarrow^{K_2} HCO_3^- + RR'NH_2^+ \tag{6}$$

The $CO_2$ permeance equation based on Eq. (6) is as follows (Li et al., 2014):

$$Q_2(p_{CO_2,0}) = \frac{D_{CO_2}}{lH_{co_2}} + \frac{D_{CO_2-X}K_2\left[\sqrt{1 + 4C_XH_{co_2}/K_2p_{CO_2,0}} - 1\right]}{2lH_{co_2}} \tag{7}$$

where $D_{CO_2}$ ($cm^2{\cdot}s^{-1}$) is $CO_2$ diffusion coefficient, $D_{CO_2-X}$ ($cm^2{\cdot}s^{-1}$) is diffusion coefficient of $CO_2$−carrier complex, $C_X$ (mol $cm^{-3}$) is carrier concentration in the AFTMs. $K_1$ and $K_2$ are the reaction equilibrium constant of Eq. (3) and Eq. (5), respectively. $l$ (cm) is the thickness of the membrane selective layer. $H_{co_2}$ (MPa $cm^3$ $mol^{-1}$) is Henry's law constant of $CO_2$, which can be calculated as a form of temperature (Chakma and Meisen, 1987),

$$H_{co_2} = \frac{exp(22.2819 - \frac{138.306\times10^2}{T} + \frac{691.346\times10^4}{T^2} - \frac{155.895\times10^7}{T^3} + \frac{120.037\times10^9}{T^4})}{7.50061} \tag{8}$$

Table 1 listed the diffusion coefficient, reaction equilibrium constant, and other simulation parameters based on the experimental results (Way and Noble, 1989).

Both Eqs. (4) and (7) derived from the two different reactions only consider the effect of gas partial pressure on the gas permeance, while in the real gas separation, the gas temperature is also another key impact factor that affects the gas permeance. Therefore, the Arrhenius equation (Safari et al., 2009) is included to explicitly describe the dependence of gas permeance to temperature, which can be presented by Eq. (9):

$$Q_{i,T} = Q_{i,T_0}exp\left[-\frac{E_p}{R}(\frac{1}{T} - \frac{1}{T_0})\right] \tag{9}$$

where $T_0$ is the reference temperature (in Kelvins), which is 298 K (25 ℃) in this study, $Q_{i,T_0}$ is determined reference gas permeance at the reference temperature, R is the molar gas constant (8.314 J $mol^{-1}$ $K^{-1}$), $E_p$ is the gas permeation activation energy, the $E_p$ value of $CO_2$ is 38.7 kJ/mol, while the $E_p$ value of $N_2$ is 62.7 kJ/mol (Han et al., 2019).

By integrating the effect of partial pressure and temperature yields:

$$Q_1(p_{CO_2,0}, T) = Q_1(p_{CO_2,0})exp\left[-\frac{E_p}{R}(\frac{1}{T} - \frac{1}{T_0})\right] \tag{10}$$

$$Q_2(p_{CO_2,0}, T) = Q_2(p_{CO_2,0})exp\left[-\frac{E_p}{R}(\frac{1}{T} - \frac{1}{T_0})\right] \tag{11}$$

Eqs. (10) and (11) can describe the effect of temperature and

**Table 1**
Diffusion coefficient and reaction equilibrium constant and other known parameters.

| Parameters | Value | Unit |
|---|---|---|
| $D_{CO_2}$ | $1 \times 10^{-8}$ | $cm^2{\cdot}s^{-1}$ |
| $D_{CO_2-X}$ | $4.34 \times 10^{-9}$ | $cm^2{\cdot}s^{-1}$ |
| $K_1$ | $1.1 \times 10^{8}$ | $cm^3$ $mol^{-1}$ |
| $K_2$ | $1.2 \times 10^{5}$ | Dimensionless |
| $l$ | $3 \times 10^{-4}$ | cm |
| $C_X$ | $8.4 \times 10^{-3}$ | mol $cm^{-3}$ |

pressure on gas permeance. However, it is believed that the reaction of $CO_2$ with hindered amines and unhindered amines takes place simultaneously in AFTMs (Zarca et al., 2017). Therefore, neither of these two equations (Eqs. (10) and (11)) can individually describe the gas permeance in AFTMs. It is believed that gas permeance is a form of a combination of those two equations. Besides, as indicated by experimental studies, water vapor in the gas stream can benefit the facilitated transport of $CO_2$ in AFTMs (Saeed and Deng, 2015; Saeed and Deng, 2016; Olivieri et al., 2017; Saeed et al., 2017). Various experimental results indicated that the gas permeance shows an exponential relationship with RH (Deng et al., 2009a; Deng et al., 2009b; Deng and Hägg, 2010). Therefore, to model for AFTMs, it is desired to include the water vapor effect (in the form of RH) in the permeance equations.

For $CO_2$, the $CO_2$ permeance as a function of RH is as follows (Deng and Hägg, 2010):

$$Q_{CO_2,RH} = Ae^{(B\times RH)} \tag{12}$$

Where A and B are factors with different values according to different membrane systems, *RH* (%) is gas RH, *RH* is usually expressed as:

$$RH = \frac{P \times x_{H_2O}}{P_{sat}} \tag{13}$$

where, $x_{H_2O}$ (%) is gas water vapor content, $P_{sat}$ (bar) is water vapor saturated pressure, $P$ (bar) is the gas pressure. $P_{sat}$ depends on the gas temperature ($T$, ℃) (Xu et al., 2019b), Buck equation (Buck, 1981) is adopted here to calculated $P_{sat}$ as it has lower at a temperature lower than 100 ℃, as shown in Eq. (14):

$$P_{sat} = 0.61121exp\left(\left(18.678 - \frac{T}{234.5}\right)\left(\frac{T}{257.14+T}\right)\right) \tag{14}$$

By integrating Eq. (12) into Eqs. (10) and (11), the gas permeance equation for AFTMs that reflects the simultaneous effects of temperature, pressure, and RH is obtained, as shown in Eqs. (15) and (16).

$$Q_1\left(p_{CO_2,0}, T, RH\right) = \left\{1 - e^{[B\times(RH-100)]}\right\}Q_1\left(p_{CO_2,0}, T\right) \tag{15}$$

$$Q_2\left(p_{CO_2,0}, T, RH\right) = e^{[B\times(RH-100)]}Q_2\left(p_{CO_2,0}, T\right) \tag{16}$$

In summary, a new gas permeance model in the form of a combination of two reactions that take place in AFTMs is proposed, as indicated as follows:

$$Q\left(T,\ p_{CO_2}, RH\right) = M \times Q_1\left(p_{CO_2,0}, T, RH\right) + N \times Q_2\left(p_{CO_2,0}, T, RH\right) \tag{17}$$

### 2.2. Variable gas permeance within the membrane module

In real membrane gas separation, RH, temperature, and partial pressure vary along the membrane during the separation process, this is particularly true when the membrane is applied to a large-scale application. In terms of the partial pressure, the partial pressure of $CO_2$ drops along the module due to permeation. RH of the gas also decreases as a result of $H_2O$ permeation. For gas temperature, as mentioned previously, JT effect is always adopted to describe the temperature decrease from the feed side to the retentate side. Eq. (18) shows the energy balance in the membrane:

$$F_{in}H_{in} + Q_c + W = F_pH_p + F_RH_R \tag{18}$$

where F indicates the molar flow rate, $Q_c$ indicates the conductive heat transfer of membrane, W is the work during the separation, H indicates the enthalpy. Subscripts *in*, *p*, and *R* represent feed side, permeate side, and retentate side, respectively. Membrane gas separation can be regarded as adiabatic and there is no work done on the system, so the Q and W are equal to zero, the energy balance equation is shown in Eq. (19).

$$F_{in}H_{in} = F_pH_p + F_RH_R \tag{19}$$

Energy balance in the form of enthalpy, the sum of permeate enthalpy and retentate enthalpy is equal to the feed enthalpy. Therefore, membrane gas separation is an isenthalpic process.

The stage cut $\theta$ is defined by:

$$\theta = \frac{F_p}{F_{in}} \tag{20}$$

From Eqs. (19) and (20), the following relation can be obtained:

$$H_{in} = (1-\theta)H_R + \theta H_p \tag{21}$$

Gorissen (Gorissen, 1987) proposed a practical method to estimate the temperature change along the membrane during the separation, the retentate temperature change can be expressed as follow:

$$T_R = T_{in} + \mu_{mix}(P_{in} - P_p)\ln(1-\theta) \tag{22}$$

$\mu_{mix}$ is the JT coefficient of permeate gas mixture, which can be calculated with molar heat capacity at constant pressure and JT coefficient $\mu_i$ of each component, as shown in Eq. (23):

$$\mu_{mix} = \frac{\sum_i^n x_iC_{p,i}\mu_i}{\sum_i^n x_iC_{p,i}} \tag{23}$$

where $C_{p,i}$ (kJ/kmol$^{-1}$·℃$^{-1}$) and $\mu_i$ (℃/bar) are the molar heat capacity at constant pressure for a pure component and JT coefficient, respectively. The value of $C_{p,i}$ and $\mu_i$ for each component is shown in Table 2 (Gorissen, 1987; Cornelissen, 1993).

## 3. Modeling experiments and results

### 3.1. Permeance equation coefficient determination

In this study, the gas permeance at various RH is fitted by Eq. (17) to calculate parameters B, M, N. Since permeance data at various RH of different AFTMs available in the literature is quite limited, hence, this study takes experimental data of PVAm/PVA membrane (Deng et al., 2009b) as an example for nonlinear curve fitting to calculate permeance equation parameters. The experiment in literature (Deng et al., 2009b) is conducted by using the feed gas contains 10 % $CO_2$ and the feed gas pressure is 2 bar while the temperature is 25℃. The sweep gas used in the experiment for better recording the permeation fluxes and gas compositions is considered to have less effect on the permeance results, thus neglected in this study. The experiment adjusted the RH of the feed gas from 50 % to 92 % by attaching a bypass line with the valve to obtain $CO_2$ permeance at various RH. The $CO_2$ permeance result (expressed in $m^3$ (STP)/$m^2$ h bar) is demonstrated as dots in Fig. 2.

As a result, it can be seen that the proposed permeance equation shows good fitting performance, the coefficient B, M, N are determined and the values are listed in Table 3.

### 3.2. Sensitivity analysis

For most gas separation applications, operating parameters (RH, $CO_2$ partial pressure, temperature) would generally decrease along the membrane due to the gas permeation. Given this circumstance, it is of importance to evaluate the effect of variations of these parameters on the gas permeance, or more precisely, the separation performance.

**Table 2**
Heat capacity at constant pressure and JT coefficient of each gas component.

| Gas compositions | $C_{p,i}$ (kJ/kmol$^{-1}$·℃$^{-1}$) | $\mu_i$ (℃/bar) |
|---|---|---|
| $CO_2$ | 37.22 | 1.016 |
| $O_2$ | 29.38 | 0.271 |
| $N_2$ | 29.09 | 0.215 |

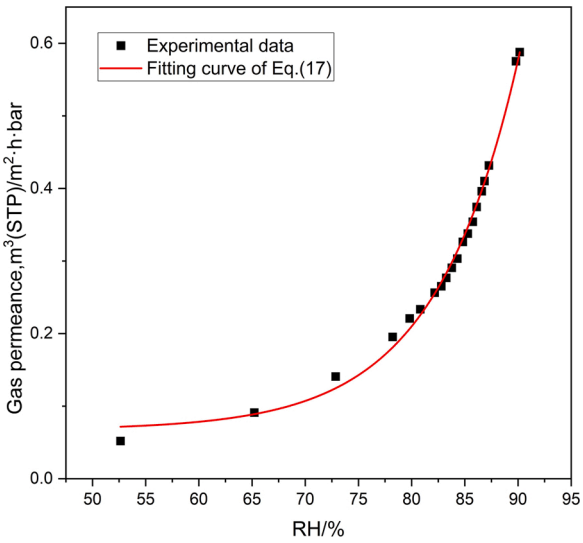


**Fig. 2.** Experimental data and fitting curves at feed gas pressure = 2.0 bar, temperature = 25℃, $CO_2$ composition = .10 %.

**Table 3**
Coefficient obtained from fitting curve results.

| Parameters | Value |
|---|---|
| B | 0.12734 |
| M | 0.23208 |
| N | 3.23837 |

Therefore, it can provide useful information for engineering design and process optimization. For this purpose, a sensitivity analysis on gas permeance to a variation of these parameters has been conducted, gas permeance results are calculated for a decrease of 5 %, 10 %, 20 %, and 30 % for each independent parameter while keeping the other two parameters unchanged, as shown in Fig. 3. All the parameters used for calculation are listed in Table 4. $Q_T$ represents variable gas permeance with temperature changes, $Q_{RH}$ represents variable permeance by the change of RH, and $Q_P$ represents the variable permeance caused by $CO_2$ partial pressure change.

From the sensitivity analysis in Fig. 3, it is clear that temperature change has the least impact on gas permeance, with a 30 % change of temperature, the gas permeance result only changes by 4.46 %. Partial pressure decrease leads to an increase of gas permeance, within a 30 %

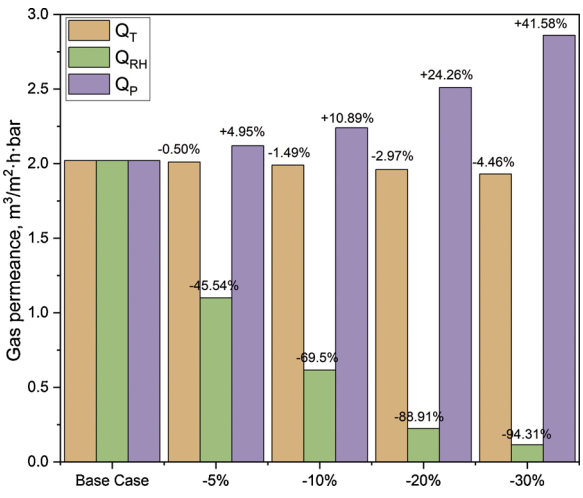


**Fig. 3.** Sensitivity analysis for different parameters effects.

**Table 4**
Parameters used for sensitivity analysis.

| Indicators | Units | Base case | −5 % Scenario | −10 % Scenario | −20 % Scenario | −30 % Scenario |
|---|---|---|---|---|---|---|
| T | ℃ | 40 | 38 | 36 | 32 | 28 |
| RH | % | 100 | 95 | 90 | 80 | 70 |
| $p_{CO_2,0}$ | bar | 0.2 | 0.19 | 0.18 | 0.16 | 0.14 |

decrease, the gas permeance will increase by around 42 %. In terms of RH, the change of RH has the most obvious effect on gas permeance than partial pressure change and temperature. With RH changing only by 10 %, the gas permeance decreases nearly half. When the RH decreases to 70 %, the gas permeance decreases by more than 90 %. In summary, RH change has the largest impact on the variation of gas permeance, followed by partial pressure change, while the temperature change brings a limited impact on gas permeance.

### 3.3. RH- and partial pressure-dependent gas permeance

As indicated in the last section, both RH and partial pressure have a pronounced effect on gas permeance. Since $CO_2$ permeance in AFTMs is a sum of the combination of Eqs. (15) and (16), it is intended to investigate the effect of various RH on gas permeance of different mechanisms. As shown in Fig. 4a. $Q_1$ represents the gas permeance that follows the mechanism without the presence of $H_2O$ (Eq. (15)), while $Q_2$ represents gas permeance under the presence of $H_2O$ (Eq. (16)). $Q_{total}$ represents the total permeance. $Q_2$ shows an increasing trend with increasing of RH, while $Q_1$ decreasing with increasing in RH. The total gas permeance is increasing with higher RH. At the RH below 80 %, gas permeance is extremely low, indicates membrane drying occurs. The results can be used to guide the membrane module design, where the membrane module area should be designed to a certain range to maintain the RH larger than 80 %. Moreover, under RH around 70 %, $Q_1$ exceeds $Q_2$, indicates that the reaction of $CO_2$ with amine carriers without the presence of $H_2O$ becomes dominant, which should be strictly prohibited. Fig. 4b presents the effect of RH on the relationship between gas permeance and partial pressure. Gas $CO_2$ composition is 10 % and the temperature is 40 ℃. It is found that increasing RH is an effective way to improve gas permeance. Gas permeance decreases with rising $CO_2$ partial pressure. However, the effect becomes less remarkable as $CO_2$ partial pressure increases.

## 4. Case study: post-combustion carbon capture simulation

To evaluate the separation performance under different operating conditions, a case study involving post-combustion carbon capture has been conducted. Single-stage membrane gas separation is adopted in this study. The $CO_2$ compositions in different exhausted flue gases may vary, gas $CO_2$ compositions from 10 % to 30 % are investigated in this study, gas specifications used in this simulation study are listed in Table 5. Flue gas entering the membrane module is saturated with water vapor at corresponding pressure and temperature to ensure the separation performance.

Eq. (17) is used to determine the variable $CO_2$ permeance, the $N_2$, $H_2O$, and $O_2$ permeance is assumed to be constant as $1.35 \times 10^{-2}$ $m^3$ (STP) $m^{-2}$ $h^{-1}$ $bar^{-1}$, 1 $m^3$ (STP) $m^{-2}$ $h^{-1}$ $bar^{-1}$, $3.37 \times 10^{-2}$ $m^3$ (STP) $m^{-2}$ $h^{-1}$ $bar^{-1}$ respectively as assumed previously (Hägg and Lindbråthen, 2005; Low et al., 2013).

### 4.1. Comparison of the proposed model and simplistic model: effect of RH, temperature and $CO_2$ partial pressure

Product $CO_2$ purity and overall recovery are two major parameters that have always been used to characterize the membrane $CO_2$ separation performance. Besides the overall recovery and permeate $CO_2$ purity,

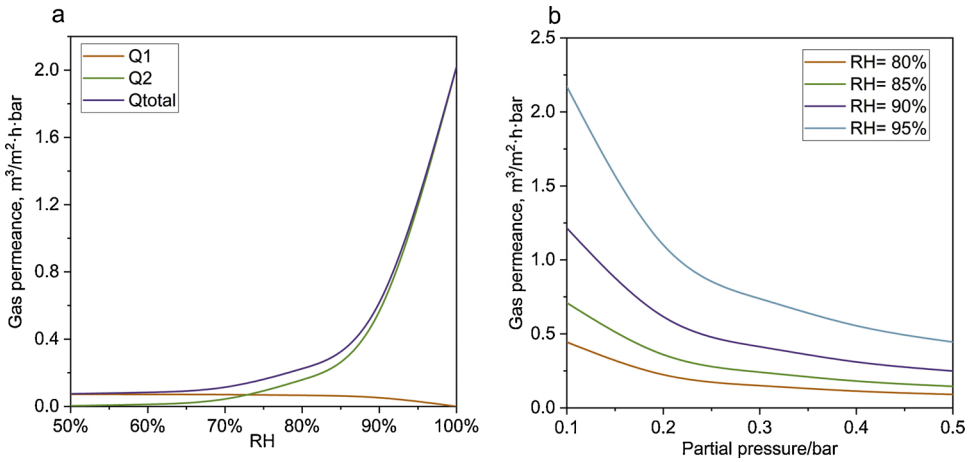


**Fig. 4.** Gas permeance at various (a) RH (b) $CO_2$ partial pressures.

**Table 5**
Gas properties used for simulation.

| Specifications | Value | Units |
|---|---|---|
| Gas flow rate | 30 | $Nm^3/h$ |
| $CO_2$ composition | 10~30 | Mol% |
| $O_2$ composition | 8 | Mol% |
| $H_2O$ composition | 1.8~7.7 | Mol% |
| $N_2$ composition | 52.3~78.2 | Mol % |
| Feed pressure | 2~5 | Bar |
| Permeate pressure | 0.5~1.25 | Bar |
| Temperature | 40~70 | ℃ |

the required membrane area is also essential to evaluate the membrane separation performance as it directly links to the cost of membrane $CO_2$ capture. This section compares the required membrane area and product purity obtained by the proposed model (solid line) and simplistic models (dash line) as a function of recovery, as shown in Fig. 5. Compared to the simplistic model that merely taking temperature and $CO_2$ partial pressure change into account in Fig. 5a, RH decline along the membrane module due to $H_2O$ permeation in the proposed model predicts approximately 100 $m^2$ higher in required membrane area and 5 % lower in product purity at largest recovery. Compared to the simplistic model that neglects the $CO_2$ partial pressure change in Fig. 5b, the proposed model predicts a lightly higher product purity and lower required membrane area, and the difference of results obtained by both models becomes more pronounced as the recovery increases. However, the difference between the proposed model and the simplistic model that does not consider JT effect is negligible, as demonstrated in Fig. 5c, implies that the temperature decrease due to JT effect brings limited impact on the separation performance of AFTMs when compared to the effect of RH and $CO_2$ partial pressure.

### 4.2. *RH profiles along the membrane at various operating conditions*

It has been investigated that gas permeance decreases as the RH decreases. In engineering design, a membrane module should be fabricated in a suitable size, and a cascade of multiple membrane modules in series is used to meet the separation requirements. Fig. 6 depicts the RH profiles along the membrane as a function of membrane area at various feed conditions. By keeping the feed pressure as 2 bar to exclude the effect of total pressure, the feed gas $CO_2$ composition varies from 10 % to 30 %. Meanwhile, a 10 % concentration of $CO_2$ with feed pressure 4 bar so to keep the same $CO_2$ partial pressure is also investigated. With the same operating pressure, the RH decreases faster with the enrichment of $CO_2$, which can be explained by the higher driving force for $CO_2$ as well as higher $CO_2$ concentration in the permeate side. Therefore, the concentration of other components like $H_2O$ in the permeate side reaches a lower value, leading to a higher driving force for $H_2O$ and a faster reduction of RH. Moreover, with a consistent $CO_2$ partial pressure (2 bar, 20 % $CO_2$ and 4 bar, 10 % $CO_2$) to exclude the impact of partial pressure, an increase of feed gas pressure from 2 bar to 4 bar leads to a faster RH decreases along the membrane module, which can be attributed to the higher driving force for $H_2O$ permeation obtained from higher feed pressure. As shown in Fig. 6b, higher operating temperature also results in a faster decrease of RH along the membrane. This is because increasing temperature slightly increases $H_2O$ permeance, a small higher $H_2O$ permeation is then obtained.

It is obvious that the RH results as a function of membrane area are far to be specific, but the results can still be used to guide the membrane module design. For example, with a required RH at 80 % for the membrane to maintain high separation performance, the largest membrane area is around 30 $m^2$ for a gas stream contains 10 % $CO_2$ under 4 bar feed gas pressure. While for 10 % $CO_2$ under 2 bar feed pressure, the largest membrane area at this operating condition is around 50 $m^2$.

### 4.3. *Temperature drop along the membrane at various operating conditions*

Fig. 7 illustrates the temperature decreases along the membrane module as a function of $CO_2$ recovery at different operating conditions. It can be observed that temperature decreases faster with an increase in product recovery. This is because $CO_2$ is the dominant permeating component and has the highest heat capacity as well as JT coefficient over other gas components, and heat is transferred from the feed side to the permeate side during $CO_2$ permeation. As shown in Fig. 7a, for a given $CO_2$ recovery with the same feed pressure 2 bar, feed gas with higher $CO_2$ concentration has a higher reduction of temperature along the membrane module. The reason is that more heat is transported to the permeate side since the gas mixture JT coefficient is higher with increasing flue gas $CO_2$ concentration. As for temperature drop under different inlet gas temperatures over a wide range of recovery shown in Fig. 7b, feed gas with higher temperature has a slightly higher decrease in temperature. However, the reduction of temperature is relatively limited as the gas permeance did not change significantly by the effect of different temperatures. Overall, the temperature drop along the membrane module over a wide range of recovery among different operating conditions is within 1.2 ℃.

### 4.4. *Partial pressure drops along the membrane at various operating conditions*

Fig. 8 demonstrates $CO_2$ partial pressure drop under various

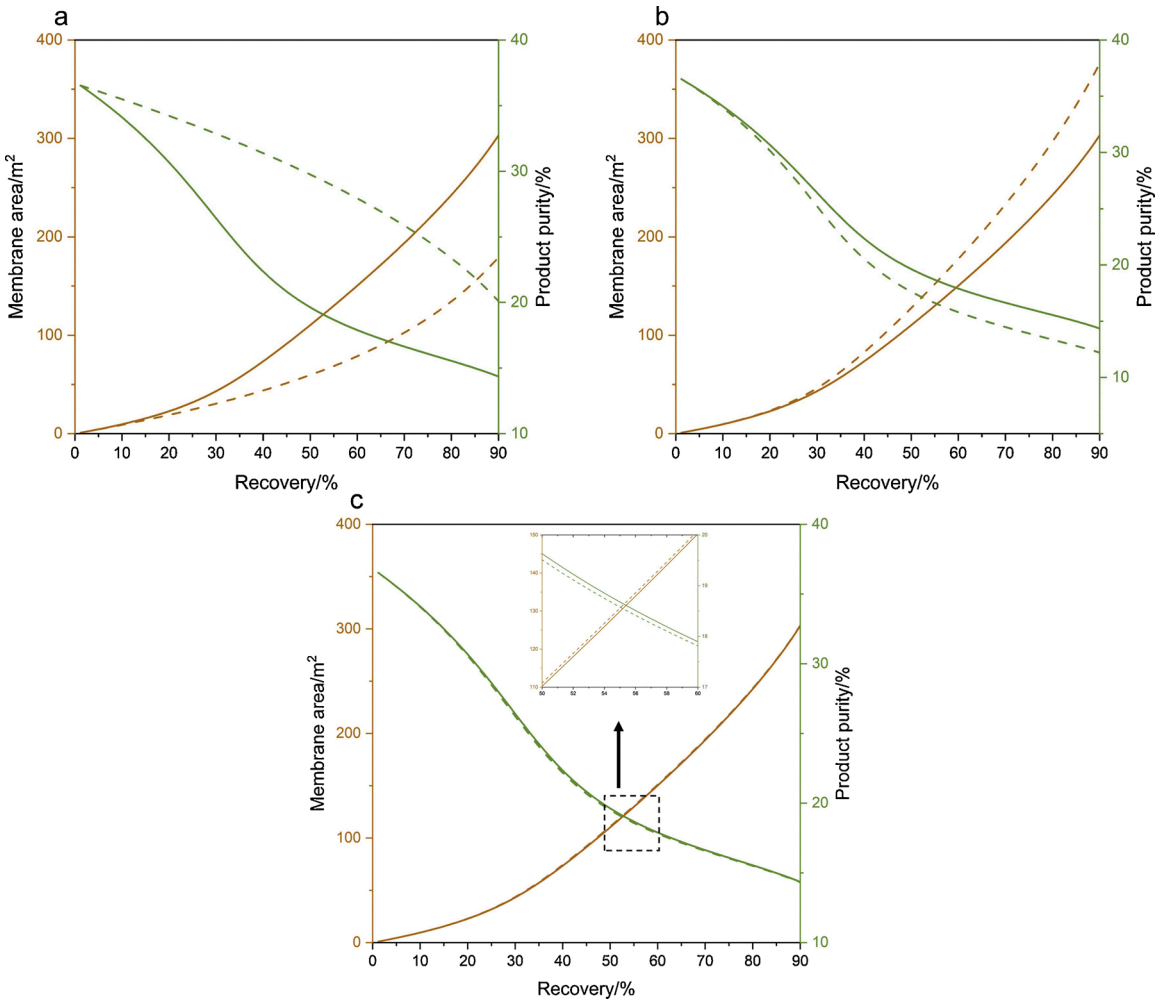


**Fig. 5.** Required membrane area and product purity as a function of recovery obtained by the proposed model (solid line) and simplistic model (dash line).

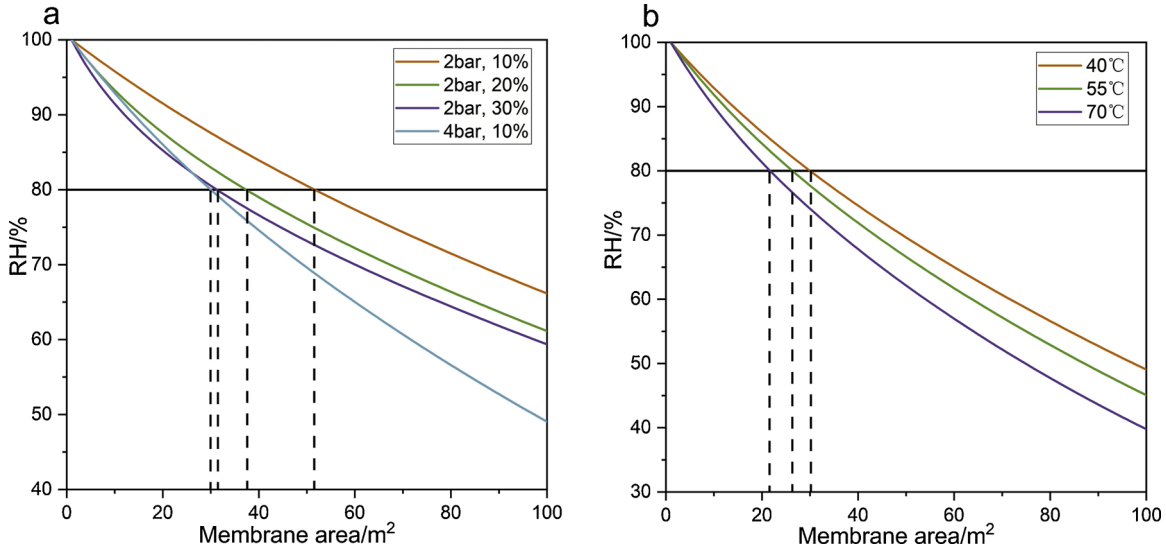


**Fig. 6.** RH as a function of membrane area at various (a) feed pressures and $CO_2$ concentrations (b) temperatures.

operating conditions. As shown in Fig. 8a, with the same inlet pressure, gas stream with higher $CO_2$ concentration has a lower $CO_2$ partial pressure drop rate, which can be explained by the RH result presented in Fig. 6a, the RH of the gas stream with higher $CO_2$ partial pressure decreases faster, resulting in lower $CO_2$ permeance as well as selectivity. Therefore, the $CO_2$ permeation of the gas stream contains higher $CO_2$ concentration becomes slower, resulting in a lower partial pressure drop rate. Elevating the feed gas total pressure while keeping $CO_2$ partial

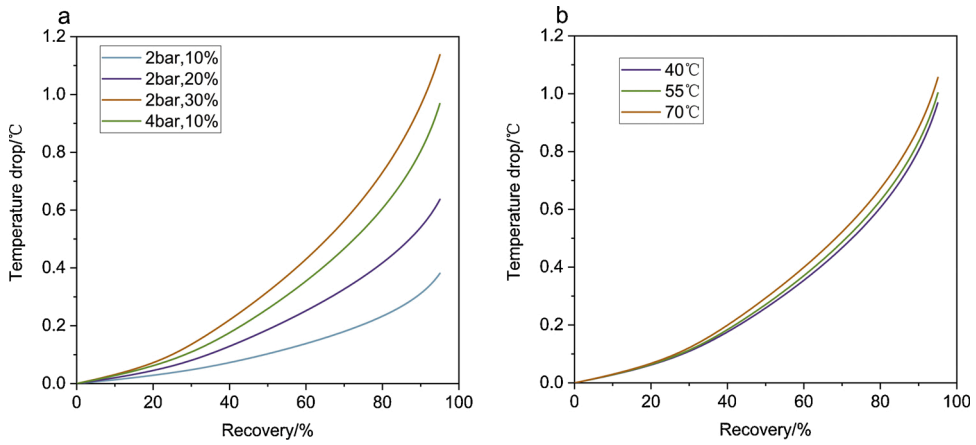


**Fig. 7.** Temperature drop along the membrane at various (a) feed pressures and $CO_2$ concentrations (b) temperatures.

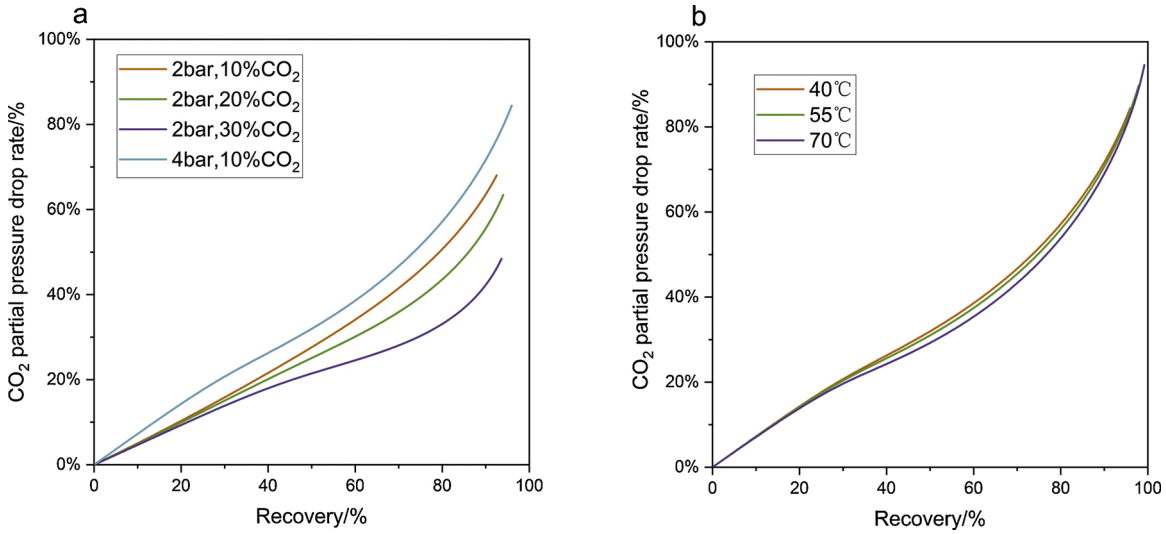


**Fig. 8.** Partial pressure drop rate at various (a) $CO_2$ concentrations and pressures (b) temperatures.

pressure the same would significantly increase the $CO_2$ partial pressure drop rate, which is because higher permeation flux is obtained at higher pressure. This indicates that feed gas pressure is the controlling factor for $CO_2$ partial pressure drop along the membrane. Interestingly, at a low recovery, $CO_2$ partial pressure drop turns to be slower with increasing recovery, while it becomes faster at a higher recovery. Because at a low recovery, RH is the controlling factor for $CO_2$ permeance and gas permeation, while at high recovery, the RH decreases to a relatively low extent and $CO_2$ partial pressure becomes the controlling factor for $CO_2$ permeance. As $CO_2$ partial pressure decreasing, the $CO_2$ permeance slightly increases, leads to a faster $CO_2$ permeation and $CO_2$ partial pressure drop. Fig. 8b indicated that higher temperature has a lower $CO_2$ partial pressure drop rate, but the difference within the different temperatures is quite limited compared to different $CO_2$ concentrations, which indicates that different operating temperatures have a minor impact on $CO_2$ partial pressure drop. Overall, the results indicate that feed pressure affects more on the $CO_2$ partial pressure changes along the membrane module.

## 5. Discussion

In this study, a new membrane gas separation model has been proposed for AFTMs. The model utilizes a gas permeance equation considering the effects of RH, temperature, and $CO_2$ partial pressure simultaneously. Sensitivity analysis suggests that the effect of RH and $CO_2$ partial pressure on gas permeance of AFTMs should not be neglected when modeling AFTMs. RH-dependent gas permeance implies that it is of importance to maintain the gas RH above 80 % for effective separation performance. Partial pressure-dependent gas permeance indicates that higher feed gas pressure is required for stable gas permeance and higher driving force, gas permeance is RH-sensitive at a high level of RH and partial pressure-sensitive at low partial pressure. However, higher operating pressure also results in a reduction of gas permeance, and requires higher energy consumption for compressors, techno-economic analysis should be further conducted to obtain the optimal operating conditions.

The effect of variable permeance on separation performance as a result of operating conditions changes along the membrane module has also been included in the model. A comparison of the proposed model and simplistic model again highlights the significance of taking the effect of RH and $CO_2$ partial pressure into account when modeling for AFTMs. Results of RH along the membrane module can be used to guide the engineering design, providing evidence for the membrane area required to maintain a high RH (80 % in this study) within the membrane module. Temperature drop along the membrane module is mainly controlled by $CO_2$ partial pressure, while $CO_2$ partial pressure drop along the membrane is mainly controlled by total feed gas pressure. Comparatively, different inlet gas temperature brings less deviation on operating conditions along the membrane as well as separation performance. However, the temperature change could be more pronounced

when separation operates at high-pressure conditions. Moreover, strategies to enhance the gas separation performance should be directed to maintaining the RH level within the membrane module or introducing gas humidification to increase the gas RH. Humidification can reduce the membrane area required for separation but increase the operating cost and energy consumption. In the future study, a techno-economic optimization analysis directed to investigate the energy consumption and economics of the overall process with humidification would be interesting.

## 6. Conclusion

This study presents a new membrane gas separation model with variable gas permeance for AFTMs. Whereas conventional models mainly consider the effect of temperature and pressure, this model enables to describe the effect of RH, temperature, and pressure simultaneously, as well as their variations along the membrane module. Sensitivity analysis and comparison of the proposed model and simplistic model emphasis the significance of considering effects of RH and $CO_2$ partial pressure for more accurate estimation on AFTMs. A case study of post-combustion carbon capture has then been involved and systematically evaluated. Results indicate that RH decreases faster with elevated partial pressure and temperature. Besides, $CO_2$ partial pressure is the controlling factor for temperature drop, while feed gas total pressure is the controlling factor for $CO_2$ partial pressure decrease. Increase in inlet gas temperature results in an insignificant variation in operating conditions along the membrane.

The preliminary results provide an insight on the modeling works on AFTMs, enabling to help in recognizing the best condition of separation as well as in providing useful information for the overall process optimization. By referring to this model, the results can be utilized to guide the membrane module as well as process design, such as humidification of the flue gas for multistage gas separation processes using AFTMs. Overall, the model proposed in this study can be integrated into the commercial process simulators to investigate the separation performance with the consideration of operating conditions changes along the membrane module, supporting the design of membrane systems for carbon capture.

## CRediT authorship contribution statement

**Qiang Yang:** Conceptualization, Methodology, Modeling, Writing - original draft. **Qianguo Lin:** Conceptualization, Methodology, Supervision, Writing - review & revision. **Xi Liang:** Conceptualization, Methodology, Writing - review & revision.

## Declaration of Competing Interest

The authors report no declarations of interest.

## Acknowledgment

The authors would like to express their gratitude for the support of the National Key R&D Program of China (No. 2017YFB0603400).

## Appendix A

Mass balance equations:

$$L_k = L_{k+1} + V_k \tag{A-1}$$

$$L_k x_{i,k} = L_{k+1} x_{i,k+1} + V_k y_{i,k} \tag{A-2}$$

Permeation flux of gas component $i$ through the membrane:

$$J_k = \sum_{i=1}^{n} Q_{i,k}(P_h x_{i,k} - P_l y_{i,k})A \tag{A-3}$$

The sum of the gas mole fractions of permeate and retentate is equal to 1:

$$\sum_{i=1}^{n} x_{i,k} = 1 \tag{A-4}$$

$$\sum_{i=1}^{n} y_{i,k} = 1 \tag{A-5}$$

For any two components $i$ and $j$:

$$\frac{y_{i,k}}{y_{j,k}} = \frac{Q_{i,k}(P_h x_{i,k} - P_l y_{i,k})}{Q_{j,k}(P_h x_{j,k} - P_l y_{j,k})} \tag{A-6}$$

$$y_{i,k} = \frac{x_{i,k} Q_{i,k} / Q_{j,k}}{r(Q_{i,k}/Q_{j,k} - 1) + x_{j,k}/y_{j,k}} \tag{A-7}$$

Replace (A-5) by (A-7):

$$y_{i,k} = \frac{x_{i,k} Q_{i,k} / Q_{j,k}}{r(Q_{i,k}/Q_{j,k} - 1) + x_{j,k}/y_{j,k}} \tag{A-8}$$

where $r = P_l/P_h$.

Newton iterative equations:

$$f(y_{j,k}) = \sum_{j=1}^{n} \frac{x_{i,k} Q_{i,k} / Q_{j,k}}{r(Q_{i,k}/Q_{j,k} - 1) + x_{j,k}/y_{j,k}} - 1 \tag{A-9}$$

$$f^{'}\left(y_{j,k}\right)=\sum_{j=1}^{n}\frac{\left(x_{i,k}Q_{i,k}/Q_{j,k}\right)x_{j,k}/{y_{j,k}}^{2}}{\left[r\left(Q_{i,k}/Q_{j,k}-1\right)+x_{j,k}/y_{j,k}\right]^{2}} \tag{A-10}$$

$$y_{j,k}^{(r+1)}=y_{j,k}^{(r)}-\frac{f\left({y_{j,k}}^{(r)}\right)}{f^{'}\left(y_{j,k}{}^{(r)}\right)} \tag{A-11}$$

Modeling solving equations

$$V_k=\frac{Q_{j,k}(P_h x_{j,k}-P_l y_{j,k})A}{y_{j,k}} \tag{A-12}$$

$$L_{k+1}=L_k-V_k \tag{A-13}$$

$$x_{i,k+1}=\frac{L_k x_{i,k}-V_k y_{i,k}}{L_k-V_k} \tag{A-14}$$

Product purity and recovery

$$y_{purity}=\frac{\sum_{k=1}^{n}y_{CO_2,k}V_k}{\sum_{k=1}^{n}V_k}\times 100\% \tag{A-15}$$

$$Re=\frac{\sum_{k=1}^{n}y_{CO_2,k}V_k}{L_1x_1}\times 100\% \tag{A-16}$$

## References


Ahmad, F., Lau, K.K., Shariff, A.M., Fong Yeong, Y., 2013. Temperature and pressure dependence of membrane permeance and its effect on process economics of hollow fiber gas separation system. J. Memb. Sci. 430, 44–55. https://doi.org/10.1016/j.memsci.2012.11.070.

Ansaloni, L., Zhao, Y., Jung, B.T., Ramasubramanian, K., Baschetti, M.G., Ho, W.S.W., 2015. Facilitated transport membranes containing amino-functionalized multi-walled carbon nanotubes for high-pressure CO2 separations. J. Memb. Sci. 490, 18–28. https://doi.org/10.1016/j.memsci.2015.03.097.

Bouton, G.R., Luyben, W.L., 2008. Optimum economie design and control of a gas permeation membrane coupled with the hydrodealkylation (HDA) process. Ind. Eng. Chem. Res. 47, 1221–1237. https://doi.org/10.1021/ie0711372.

Brunetti, A., Scura, F., Barbieri, G., Drioli, E., 2010. Membrane technologies for CO2 separation. J. Memb. Sci. 359, 115–125. https://doi.org/10.1016/j.memsci.2009.11.040.

Buck, A.L., 1981. New equations for computing vapor pressure and enhancement factor. J. Appl. Meteorol. Climatol. 20, 1527–1532.

Caplow, M., 1968. Kinetics of carbamate formation and breakdown. J. Am. Chem. Soc. 90, 6795–6803. https://doi.org/10.1021/ja01026a041.

Chakma, A., Meisen, A., 1987. Solubility of CO2 in aqueous methyldiethanolamine and N,N-Bis(hydroxyethyl)piperazine solutions. Ind. Eng. Chem. Res. 26, 2461–2466. https://doi.org/10.1021/ie00072a013.

Coker, D.T., Freeman, B.D., Fleming, G.K., 1998. Modeling multicomponent gas separation using hollow-fiber membrane contactors. AIChE J. 44, 1289–1302. https://doi.org/10.1002/aic.690440607.

Cornelissen, A.E., 1993. Heat effect in gas permeation, with special reference to spiral-wound modules. J. Memb. Sci. 76, 185–192. https://doi.org/10.1016/0376-7388(93)85216-J.

Danckwerts, P.V., 1979. The reaction of CO2 with ethanolamines. Chem. Eng. Sci. 34, 443–446. https://doi.org/10.1016/0009-2509(79)85087-3.

Deng, L., Hägg, M.B., 2010. Swelling behavior and gas permeation performance of PVAm/PVA blend FSC membrane. J. Memb. Sci. 363, 295–301. https://doi.org/10.1016/j.memsci.2010.07.043.

Deng, L., Kim, T.-J., Sandru, M., Hägg, M.-B., 2009a. PVA/PVAm blend FSC membrane for natural gas sweetening. In: Proceedings of the 1st Annual Gas Processing Symposium. Elsevier Ltd., 1st ed. https://doi.org/10.1016/b978-0-444-53292-3.50032-8.

Deng, L., Kim, T.J., Hägg, M.B., 2009b. Facilitated transport of CO2 in novel PVAm/PVA blend membrane. J. Memb. Sci. 340, 154–163. https://doi.org/10.1016/j.memsci.2009.05.019.

Ebadi Amooghin, A., Moftakhari Sharifzadeh, M.M., Zamani Pedram, M., 2018. Rigorous modeling of gas permeation behavior in facilitated transport membranes (FTMs); evaluation of carrier saturation effects and double-reaction mechanism. Greenh. Gases Sci. Technol. 8, 429–443. https://doi.org/10.1002/ghg.1750.

Friedlander, S.K., Keller, K.H., 1965. Mass transfer in reacting systems near equilibrium. Use of the affinity function. Chem. Eng. Sci. 20, 121–129. https://doi.org/10.1016/0009-2509(65)85005-9.

Gorissen, H., 1987. Temperature changes involved in membrane gas separations. Chem. Eng. Process. 22, 63–67. https://doi.org/10.1016/0255-2701(87)80032-6.

Guandalini, G., Romano, M.C., Ho, M., Wiley, D., Rubin, E.S., Abanades, J.C., 2019. A sequential approach for the economic evaluation of new CO2 capture technologies for power plants. Int. J. Greenh. Gas Control 84, 219–231. https://doi.org/10.1016/j.ijggc.2019.03.006.

Hägg, M.B., Lindbråthen, A., 2005. CO2 capture from natural gas fired power plants by using membrane technology. Ind. Eng. Chem. Res. 44, 7668–7675. https://doi.org/10.1021/ie050174v.

Han, Y., Ho, W.S.W., 2018. Recent advances in polymeric membranes for CO2 capture. Chinese J. Chem. Eng. 26, 2238–2254. https://doi.org/10.1016/j.cjche.2018.07.010.

Han, Y., Wu, D., Ho, W.S.W., 2019. Simultaneous effects of temperature and vacuum and feed pressures on facilitated transport membrane for CO2/N2 separation. J. Memb. Sci. 573, 476–484. https://doi.org/10.1016/j.memsci.2018.12.028.

Hosseini, S.S., Dehkordi, J.A., Kundu, P.K., 2016. Gas permeation and separation in asymmetric hollow fiber membrane permeators: mathematical modeling, sensitivity analysis and optimization. Korean J. Chem. Eng. 33, 3085–3101. https://doi.org/10.1007/s11814-016-0198-z.

Katoh, T., Tokumura, M., Yoshikawa, H., Kawase, Y., 2011. Dynamic simulation of multicomponent gas separation by hollow-fiber membrane module: nonideal mixing flows in permeate and residue sides using the tanks-in-series model. Sep. Purif. Technol. 76, 362–372. https://doi.org/10.1016/j.seppur.2010.11.006.

Lee, S., Binns, M., Lee, J.H., Moon, J.H., Yeo, Jgu, Yeo, Y.K., Lee, Y.M.M., Kim, J.K., 2017. Membrane separation process for CO2 capture from mixed gases using TR and XTR hollow fiber membranes: process modeling and experiments. J. Memb. Sci. 541, 224–234. https://doi.org/10.1016/j.memsci.2017.07.003.

Li, S., Wang, Z., He, W., Zhang, C., Wu, H., Wang, J., Wang, S., 2014. Effects of minor SO2 on the transport properties of fixed carrier membranes for CO2 capture. Ind. Eng. Chem. Res. 53, 7758–7767. https://doi.org/10.1021/ie404063r.

Low, B.T., Zhao, L., Merkel, T.C., Weber, M., Stolten, D., 2013. A parametric study of the impact of membrane materials and process operating conditions on carbon capture from humidified flue gas. J. Memb. Sci. 431, 139–155. https://doi.org/10.1016/j.memsci.2012.12.014.

N.Borhani, T., Wang, M., 2019. Role of solvents in CO2 capture processes: the review of selection and design methods. Renew. Sustain. Energy Rev. 114, 109299 https://doi.org/10.1016/j.rser.2019.109299.

Ohs, B., Falkenberg, M., Wessling, M., 2019. Optimizing hybrid membrane-pressure swing adsorption processes for biogenic hydrogen recovery. Chem. Eng. J. 364, 452–461. https://doi.org/10.1016/j.cej.2019.01.136.

Olivieri, L., Aboukeila, H., Giacinti Baschetti, M., Pizzi, D., Merlo, L., Sarti, G.C., 2017. Humid permeation of CO2 and hydrocarbons in Aquivion® perfluorosulfonic acid ionomer membranes, experimental and modeling. J. Memb. Sci. 542, 367–377. https://doi.org/10.1016/j.memsci.2017.08.030.

Pan, C.Y., 1983. Gas separation by permeators with high-flux asymmetric membranes. AIChE J. 29, 545–552. https://doi.org/10.1002/aic.690290405.

Paul, D.R., Koros, W.J., 1976. Effect of partially immobilizing sorption on permeability and the diffusion time lag. J. Polym. Sci. Part A-2 Polym. Phys. 14, 675–685. https://doi.org/10.1002/pol.1976.180140409.

Pfister, M., Belaissaoui, B., Favre, E., 2017. Membrane gas separation processes from wet postcombustion flue gases for carbon capture and use: a critical reassessment. Ind. Eng. Chem. Res. 56, 591–602. https://doi.org/10.1021/acs.iecr.6b03969.

Rautenbach, R., Dahm, W., 1987. Oxygen and methane enrichment — a comprison of module arrangements in gas permeation. Chem. Eng. Technol. 10, 256–261. https://doi.org/10.1002/ceat.270100131.

Robeson, L.M., 2008. The upper bound revisited. J. Memb. Sci. 320, 390–400. https://doi.org/10.1016/j.memsci.2008.04.030.

Rodrigues, S.C., Sousa, J., Mendes, A., 2018. Facilitated transport membranes for CO2/H2 separation. Current Trends and Future Developments on (Bio-) Membranes: Carbon Dioxide Separation/Capture by Using Membranes. Elsevier, pp. 359–384. https://doi.org/10.1016/B978-0-12-813645-4.00013-1.

Saeed, M., Deng, L., 2015. CO2 facilitated transport membrane promoted by mimic enzyme. J. Memb. Sci. 494, 196–204. https://doi.org/10.1016/j.memsci.2015.07.028.

Saeed, M., Deng, L., 2016. Carbon nanotube enhanced PVA-mimic enzyme membrane for post-combustion CO2 capture. Int. J. Greenh. Gas Control 53, 254–262. https://doi.org/10.1016/j.ijggc.2016.08.017.

Saeed, M., Rafiq, S., Bergersen, L.H., Deng, L., 2017. Tailoring of water swollen PVA membrane for hosting carriers in CO2 facilitated transport membranes. Sep. Purif. Technol. 179, 550–560. https://doi.org/10.1016/j.seppur.2017.02.022.

Safari, M., Ghanizadeh, A., Montazer-Rahmati, M.M., 2009. Optimization of membrane-based CO2-removal from natural gas using simple models considering both pressure and temperature effects. Int. J. Greenh. Gas Control 3, 3–10. https://doi.org/10.1016/j.ijggc.2008.05.001.

Scholz, M., Harlacher, T., Melin, T., Wessling, M., 2013. Modeling gas permeation by linking nonideal effects. Ind. Eng. Chem. Res. 52, 1079–1088. https://doi.org/10.1021/ie202689m.

Shao, P., Dal-Cin, M., Kumar, A., Li, H., Singh, D.P., 2012. Design and economics of a hybrid membrane-temperature swing adsorption process for upgrading biogas. J. Memb. Sci. 413–414, 17–28. https://doi.org/10.1016/j.memsci.2012.02.040.

Shindo, Y., Hakuta, T., Yoshitome, H., 1985. Calculation methods for multicomponent gas separation by permeation. Sep. Sci. Technol. 20, 445–459. https://doi.org/10.1080/01496398508060692.

Siagian, U.W.R., Raksajati, A., Himma, N.F., Khoiruddin, K., Wenten, I.G., 2019. Membrane-based carbon capture technologies: membrane gas separation vs. membrane contactor. J. Nat. Gas Sci. Eng. 67, 172–195. https://doi.org/10.1016/j.jngse.2019.04.008.

Song, C., Sun, Y., Fan, Z., Liu, Q., Ji, N., Kitamura, Y., 2018. Parametric study of a novel cryogenic-membrane hybrid system for efficient CO2 separation. Int. J. Greenh. Gas Control 72, 74–81. https://doi.org/10.1016/j.ijggc.2018.03.009.

Song, C., Liu, Q., Deng, S., Li, H., Kitamura, Y., 2019. Cryogenic-based CO2 capture technologies: state-of-the-art developments and current challenges. Renew. Sustain. Energy Rev. 101, 265–278. https://doi.org/10.1016/j.rser.2018.11.018.

Soroodan Miandoab, E., Kentish, S.E., Scholes, C.A., 2020. Non-ideal modelling of polymeric hollow-fibre membrane systems: pre-combustion CO2 capture case study. J. Memb. Sci. 595, 117470. https://doi.org/10.1016/j.memsci.2019.117470.

Tomé, L.C., Gouveia, A.S.L., Freire, C.S.R., Mecerreyes, D., Marrucho, I.M., 2015. Polymeric ionic liquid-based membranes: influence of polycation variation on gas transport and CO2 selectivity properties. J. Memb. Sci. 486, 40–48. https://doi.org/10.1016/j.memsci.2015.03.026.

Tong, Z., Vakharia, V.K., Gasda, M., Ho, W.S.W., 2015. Water vapor and CO2 transport through amine-containing facilitated transport membranes. React. Funct. Polym. 86, 111–116. https://doi.org/10.1016/j.reactfunctpolym.2014.09.010.

Wang, J., Wang, S., Xin, Q., Li, Y., 2017. Perspectives on water-facilitated CO2 capture materials. J. Mater. Chem. A 5, 6794–6816. https://doi.org/10.1039/c7ta01297g.

Way, J.D., Noble, R.D., 1989. Competitive facilitated transport of acid gases in perfluorosulfonic acid membranes. J. Memb. Sci. 46, 309–324. https://doi.org/10.1016/S0376-7388(00)80342-7.

Xu, J., Wang, Z., Qiao, Z., Wu, H., Dong, S., Zhao, S., Wang, J., 2019a. Post-combustion CO2 capture with membrane process: practical membrane performance and appropriate pressure. J. Memb. Sci. 581, 195–213. https://doi.org/10.1016/j.memsci.2019.03.052.

Xu, J., Wang, Z., Qiao, Z., Wu, H., Dong, S., Zhao, S., Wang, J., 2019b. Post-combustion CO2 capture with membrane process: practical membrane performance and appropriate pressure. J. Memb. Sci. 581, 195–213. https://doi.org/10.1016/j.memsci.2019.03.052.

Yang, D., Ren, H., Li, Y., Wang, Z., 2017. Suitability of cross-flow model for practical membrane gas separation processes. Chem. Eng. Res. Des. 117, 376–381. https://doi.org/10.1016/j.cherd.2016.10.036.

Yang, Q., Lin, Q., Sammarchi, S., Li, J., Li, S., Wang, D., 2020. Water vapor effects on CO2 separation of amine-containing facilitated transport membranes (AFTMs) module: mathematical modeling using tanks-in-series approach. Greenh. Gases Sci. Technol. 17, 1–17. https://doi.org/10.1002/ghg.2031.

Zarca, R., Ortiz, A., Gorri, D., Ortiz, I., 2017. A practical approach to fixed-site-carrier facilitated transport modeling for the separation of propylene/propane mixtures through silver-containing polymeric membranes. Sep. Purif. Technol. 180, 82–89. https://doi.org/10.1016/j.seppur.2017.02.050.